

Investigating Long-term Training for Remote Sensing Object Detection

JongHyun Park¹, Yechan Kim^{1*}, Moongu Jeon^{1*}

¹Machine Learning and Vision Laboratory, Gwangju Institute of Science and Technology (GIST), Gwangju, 61005, Republic of Korea.

*Corresponding author(s). E-mail(s): yechankim@gm.gist.ac.kr;
mgjeon@gist.ac.kr;

Contributing authors: citizen135@gm.gist.ac.kr;

Abstract

Recently, numerous methods have achieved impressive performance in remote sensing object detection, relying on convolution or transformer architectures. Such detectors typically have a feature backbone to extract useful features from raw input images. A common practice in current detectors is initializing the backbone with pre-trained weights available online. Fine-tuning the backbone is typically required to generate features suitable for remote-sensing images. While the prolonged training could lead to over-fitting, hindering the extraction of basic visual features, it can enable models to gradually extract deeper insights and richer representations from remote sensing data. Striking a balance between these competing factors is critical for achieving optimal performance. In this study, we aim to investigate the performance and characteristics of remote sensing object detection models under very long training schedules, and propose a novel method named Dynamic Backbone Freezing (DBF) for feature backbone fine-tuning on remote sensing object detection under long-term training. Our method addresses the dilemma of whether the backbone should extract low-level generic features or possess specific knowledge of the remote sensing domain, by introducing a module called ‘Freezing Scheduler’ to manage the update of backbone features during long-term training dynamically. Extensive experiments on DOTA and DIOR-R show that our approach enables more accurate model learning while substantially reducing computational costs in long-term training. Besides, it can be seamlessly adopted without additional effort due to its straightforward design. The code is available at <https://github.com/unique-chan/dbf>.

Keywords: Remote sensing object detection, long-term training, fine-tuning, backbone freezing

1 Introduction

The rapid advancement of geospatial and deep learning technologies has revolutionized remote sensing object detection, enabling significant improvements in accuracy and efficiency. Modern object detectors rely on a feature backbone such as convolutional neural networks and transformer architectures to extract meaningful representations from raw input images [1–3]. These backbone models typically benefit from pre-trained weights on large-scale datasets such as ImageNet [4], which serve as a foundation for learning low-level features like edges and textures. Fine-tuning these pre-trained backbones with remote sensing datasets is a common practice to adapt to the unique characteristics of aerial and satellite imagery.

However, the process of fine-tuning under long-term training schedules introduces unique challenges and opportunities for remote sensing object detection. On the one hand, prolonged training can lead to overfitting, especially in feature backbones, hindering the extraction of fundamental visual features critical for generalization. On the other hand, such extended schedules provide a valuable opportunity to acquire domain-specific and enriched knowledge from data, potentially enhancing the model’s ability to detect intricate patterns unique to remote sensing imagery. For example, Beyer et al. [5] empirically found that prolonged training with appropriate data augmentation strategies may be important to achieve better accuracy. This trade-off between preserving generic features and specializing for the domain presents a critical challenge in designing effective training strategies for feature backbones.

In addition, many modern object detection models are released with pre-trained weights based on natural image datasets such as ImageNet. To adapt these models to remote sensing tasks, fine-tuning is essential; however, as the model size increases, this process becomes increasingly resource-intensive. In particular, training large backbones from scratch or even fully fine-tuning them requires substantial GPU memory and computation time, which can hinder practical deployment in remote sensing scenarios [6–8].

To tackle this limitation, we introduce a novel feature backbone fine-tuning method named **DBF** (Dynamic Backbone Freezing) for remote sensing object detection under long-term training. Our primary objective is to examine the performance and behavioral traits of remote sensing object detection models when subjected to prolonged training schedules with our fine-tuning approach. Inspired by recent studies of fine-tuning with frozen settings in natural language processing (e.g. [9–12]), we aim to address the dilemma of whether the backbone should extract low-level generic features or specialize in domain-specific knowledge of remote sensing. Intuitively, we implement a module named ‘Freezing Scheduler’ to dynamically control the update of the feature backbone for each epoch during training as shown in Fig. 1. The backbone receives knowledge concerning the downstream remote sensing data when the Freezing Scheduler sends a signal to open the backward route. Otherwise, the backbone becomes frozen, keeping the knowledge preserved while decreasing the computational complexity. Extensive experiments on DOTA [13] and DIOR-R [14] prove that our alternately freezing scheme can achieve better accuracy while significantly reducing GPU memory usage and training time, as indicated in Fig. 2 and Table 2.

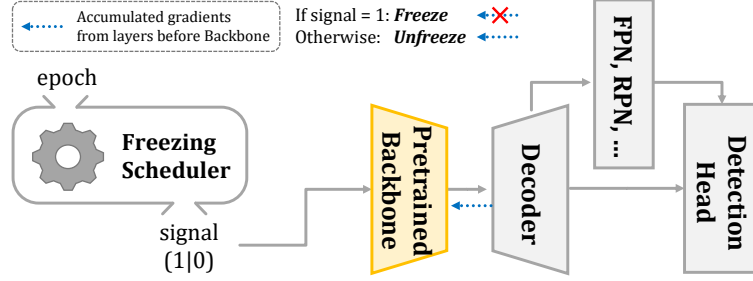


Fig. 1 Illustration of training remote sensing object detectors with the proposed framework named Dynamic Backbone Freezing (DBF). DBF allows the backbone to receive knowledge from the downstream data when Freezing Scheduler sends a signal to open the backward route. This ensures robust prediction by preventing over-fitting while also significantly saving training costs.

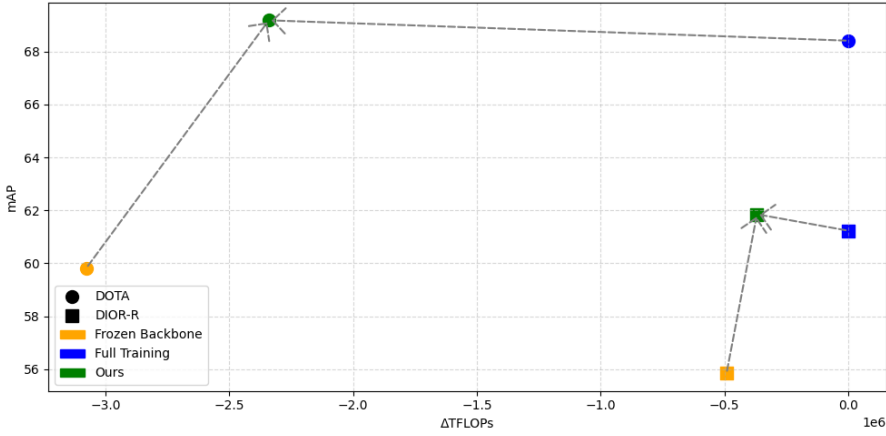


Fig. 2 Impact of the proposed method on remote sensing object detection. The above visualization indicates the performance of DOTA and DIOR-R benchmark datasets using models using FCOS with ResNet-50. Under long-term training, our method achieves the highest prediction accuracy (mAP) while significantly reducing computational costs (FLOPs), compared to existing methods. Besides FCOS, Faster R-CNN and RetinaNet also show similar trends.

The main contributions of this work are as follows:

- We present DBF (Dynamic Backbone Freezing), a novel fine-tuning strategy that enables efficient adaptation of pre-trained models to the remote sensing domain under long-term training scenarios.
- DBF significantly reduces training cost—such as GPU memory usage and FLOPs—while preserving or even enhancing detection performance, especially for large-scale models for remote sensing object detection.
- The design of DBF is simple and framework-agnostic, ensuring seamless integration into existing remote sensing object detection models.
- We conduct extensive experiments on two well-known benchmarks for remote sensing object detection, including DOTA and DIOR-R, demonstrating that DBF achieves consistent gains over both full training and frozen-backbone baselines.

The remainder of this paper is organized as follows: Section 2 reviews related work to provide context and highlight the contributions of this study. Section 3 introduces the proposed methodology, including the design and implementation of DBF. Section 4 and 5 present experimental results and a detailed analysis of the method’s performance. Finally, Section 6 concludes the study and outlines potential directions for future research.

2 Related work

2.1 Pre-training and fine-tuning for remote sensing object detection

Unlike natural scene images in datasets such as ImageNet, remote sensing images often exhibit distinct domain characteristics, including small object sizes, low contrast, and degradation caused by atmospheric or sensor-related conditions such as haze, fog, and rain. These factors substantially hinder detection accuracy, making image enhancement and restoration critical pre-processing steps.

Nevertheless, even with enhanced input quality, domain-specific fine-tuning remains essential, as feature backbones pre-trained on natural image datasets still require adaptation to effectively capture the unique spatial and spectral characteristics of remote sensing scenes.

Modern deep learning-based object detectors usually include a feature backbone to extract key features for downstream tasks from the raw input images. For object detection on natural scenes, it becomes a de facto standard to initialize the backbone with pretraining on ImageNet [4] over the years, as it is one of the largest databases in visual object recognition, enabling models to learn a broad spectrum of features such as edges, textures, and shapes. Interestingly, the same research trend to use ImageNet pre-trained weights for the backbone has been observed in the remote sensing community for the following reasons. (i) Aerial and satellite imagery datasets often face challenges including limited diversity and scale due to geopolitical reasons, security concerns, and cost issues. For example, Wang et al. [15] discovered the inefficiency of solely leveraging remote sensing images for detection and segmentation tasks. (ii) There exists an implicit consensus that though remote sensing imagery and natural scene images have different characteristics, they may still share some common visual patterns. (iii) ImageNet pre-trained weights are readily accessible through various deep learning frameworks online available.

Fine-tuning the backbone with datasets for downstream remote sensing tasks is a common strategy to bridge the knowledge gap between natural and remote sensing scenes, yet it may impede overall low-level feature extraction due to the domain-restricted remote sensing data, limiting performance enhancement. Hence, several researchers have concentrated on advanced remote sensing pre-training (e.g. [16–22]).

For instance, the benefits of large unlabeled datasets for pre-training with masked autoencoding have been demonstrated [16]. Robust representations for remote sensing understanding can be learned by simultaneously acquiring general knowledge from natural images via supervised learning and domain-specific knowledge from remote sensing images through self-supervised learning [19]. Multi-task pre-training has also

been introduced to construct remote sensing foundation models [20]. Semi-supervised object detection using uncurated data has been proposed [23]. A transformation-invariant few-shot detection model improves generalization in limited data regimes [24]. Point-level supervision significantly reduces annotation cost while maintaining segmentation accuracy [25].

However, we argue that the effectiveness of such pretraining strategies is still restricted in long-term training because the weights of the backbone heavily shift further from the initial pre-trained values. To mitigate this issue, we focus on designing a feature backbone fine-tuning method for remote sensing object detection under long-term training schemes.

2.2 Freezing backbones in deep learning

The frozen setting in NLP (Natural Language Processing), particularly in the context of large language models, refers to a technique where pre-trained models are used without updating their parameters for other downstream tasks. This research trend has gained attention for its efficiency and effectiveness in various applications. One significant research branch is the exploration of parameter-efficient fine-tuning methods. These techniques aim to fine-tune backbone models with a minimal number of additional parameters. For example, Adapters [9], small and trainable modules, are designed to be inserted within each layer of the pre-trained model. These are fine-tuned on specific tasks while keeping the majority of the model parameters frozen. On the other hand, Prefix-tuning [10] adds task-specific prefixes to the input tokens, allowing the model to adjust its behavior for different tasks without modifying the core model parameters. Moreover, LoRA [11] decomposes weight matrices into low-rank representations, updating only the low-rank components during fine-tuning.

In addition, recent efforts have focused on enhancing detection performance while reducing computational complexity by eliminating attention mechanisms. For example, Gao et al. [26] propose an attention-free global multiscale fusion network tailored for remote sensing object detection, demonstrating efficient feature extraction without the computational overhead of self-attention.

Beyond parameter-efficient tuning strategies, some researchers have explored alternative architectures inspired by neuromorphic computing. For instance, Li et al. [27] present a spiking neural network-based object detector, significantly reducing energy consumption while maintaining detection performance. Such approaches align with the increasing demand for lightweight and efficient models in resource-constrained remote sensing environments.

In computer vision, the usual practice for dense prediction tasks such as detection and segmentation had been to incorporate extra networks to avoid losing information in the feature backbone during fine-tuning (e.g. [28, 29]). After the success of the frozen setting in NLP, this concept has influenced research in computer vision tasks as well. Lin et al. [30] involves utilizing frozen pre-trained networks, with a task-specific head network to be fine-tuned for downstream tasks. Interestingly, Vasconcelos et al. [31] presents a fine-training scheme for detectors not to update the ImageNet-pretrained backbone. This simple strategy enables models to achieve competitive performance while significantly reducing resource usage for generic object detection on natural

scenes. However, to our knowledge, only a few have focused on the frozen setting in the same context for remote sensing understanding. Therefore, in this paper, we revisit the frozen setting for remote sensing object detection.

2.3 Recent object detection paradigm for remote sensing

Oriented object detection refers to a specialized task where the goal is to locate and classify objects in an image while accounting for their orientation (rotation). Unlike traditional object detection, which uses AABBs (Axis-Aligned Bounding Boxes) to enclose objects, oriented object detection employs OBBs (Oriented Bounding Boxes) that align with the object’s true orientation in the image [32].

Traditionally, convolution neural network-based oriented object detectors can be broadly classified into two categories: one-stage methods and two-stage methods. One-stage object detection methods frame object detection as a single regression problem. These models directly predict class probabilities and bounding box coordinates from feature maps, bypassing the need for a region proposal stage. By optimizing detection end-to-end, one-stage detectors achieve significantly faster inference speeds, making them highly suitable for real-time applications. Traditionally, these methods employ anchor-based mechanisms, where predefined anchor boxes of various scales and aspect ratios guide the network to predict bounding boxes. While efficient, anchor-based one-stage detectors can suffer from challenges such as anchor design sensitivity. To address this, anchor-free one-stage detectors, such as FCOS [33], Oriented Rep [34], and CFA [35], propose bounding boxes by directly predicting object center points or key points, eliminating the dependency on predefined anchors. Two-stage object detection methods, typified by the R-CNN family (e.g., Faster R-CNN [36], Oriented R-CNN [37] and ReDet [38]), follow a decoupled pipeline. The first stage generates candidate region proposals (via an RPN in anchor-based methods), while the second stage refines these proposals and predicts class labels. Anchor-based two-stage detectors have long been the standard, with their region proposal networks relying on anchors to localize potential objects effectively.

Recently, transformer-based methods have emerged as a groundbreaking approach in object detection, shifting the paradigm from traditional convolutional designs to sequence modeling. These models leverage self-attention mechanisms and end-to-end optimization, as seen in DETR (DEtection TRansformer) [39] and Deformable DETR [40]. CLT-DETR [41] is the first adaptation of DETR for oriented object detection. AO2-DETR [42] enhances Deformable DETR by introducing an oriented box generation and refinement module, improving localization accuracy. D2Q-DETR [43] further refines this paradigm with dynamic queries that reduce object tokens progressively, balancing accuracy and efficiency. OrientedFormer [3] introduces Gaussian positional encoding, Wasserstein self-attention, and oriented cross-attention to detect arbitrarily oriented objects in remote sensing images.

Building upon these advances, recent studies have explored efficient backbone architectures tailored to ultra-high-resolution remote sensing imagery. DynamicVis [44] proposes a selective state-space backbone that adaptively attends to informative regions while suppressing less relevant areas. This design achieves high performance

with lower complexity than traditional transformer-based models, offering a promising direction for scalable and generalizable remote sensing backbones.

In addition, visual foundation models have been increasingly adopted to adapt large-scale pre-trained vision backbones to remote sensing tasks. Rather than full model retraining, these approaches often utilize efficient fine-tuning strategies. For example, RSPrompter [45] builds on the Segment Anything Model (SAM), incorporating LoRA-based prompt learning for parameter-efficient instance segmentation. Similarly, RSRefSeg2 [46] introduces a CLIP-SAM integrated framework with dual-stage referring prompts for open-vocabulary segmentation. These methods demonstrate that with appropriate prompt design and cross-modal alignment, visual foundation models can be flexibly and efficiently adapted to a wide range of remote sensing applications.

3 Proposed approach

In this section, we introduce a simple, but efficient feature backbone fine-tuning method namely Dynamic Backbone Fine-tuning (DBF) for remote sensing object detection, particularly in long-term training.

3.1 Motivation

Compared to the existing freezing methods like [31], which adopt a static freezing strategy, our approach introduces dynamic adjustments to the trainability of backbone parameters during training. This innovation enables the model to effectively balance two competing objectives in remote sensing object detection: (i) generic feature extraction, which ensures robust generalization across diverse input types (- by unfreezing -), and (ii) domain-specific feature extraction, which facilitates accurate and specialized predictions (- by freezing -). Previous approaches, such as [31], often adopt a static freezing mechanism where the backbone remains either completely trainable or entirely frozen throughout the training process. While this reduces computational overhead, it may fail to effectively balance generalization and specialization. Fully frozen backbones risk underfitting to domain-specific characteristics, while fully trainable backbones may lose essential low-level generic features from pre-trained weights.

In this study, ‘long-term’ training refers to schedules extending beyond 200 epochs, allowing models to gradually acquire enriched domain-specific knowledge while preserving generic features through DBF. In existing papers, the models are usually trained for 12 epochs with remote sensing object detection benchmarks such as DOTA and DIOR-R [47].

3.2 Overview of Dynamic Backbone Freezing

In this work, we propose a simple but efficient feature backbone fine-tuning method for remote sensing object detection. Our training scheme enables the model to preserve the initialized low-level generic features from natural images while harmoniously acquiring specialized knowledge in remote sensing. This is achieved by alternately freezing and unfreezing the backbone using the ‘Freezing Scheduler’ controller.

More precisely, DBF inherently aligns with the dual objectives by:

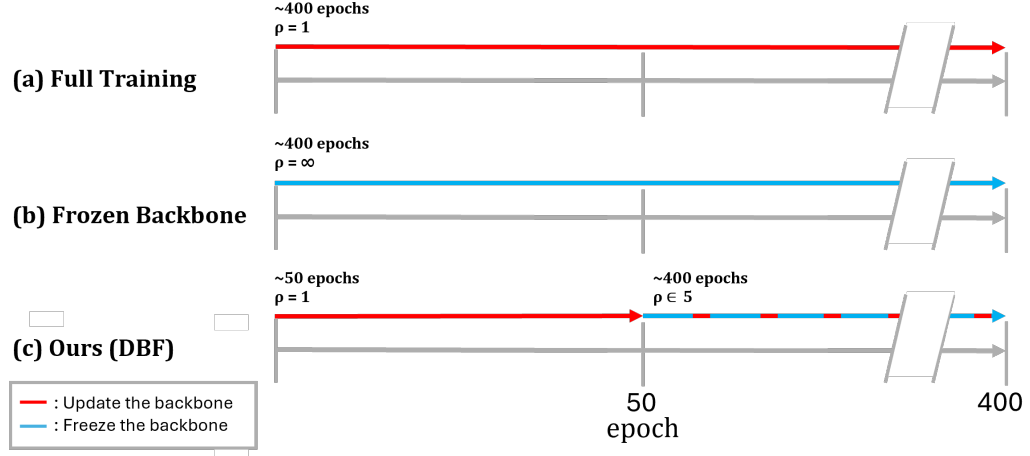


Fig. 3 Visual illustration of long-term training strategies for remote sensing object detection over 400 epochs: (a) Full Training, (b) Frozen Backbone, (c) Ours (DBF).

- Freezing the backbone to prioritize generalization and prevent overfitting to limited domain-specific data.
- Unfreezing the backbone intermittently to allow fine-tuning on specialized features as the training progresses and domain-specific patterns become more apparent.

The detail of **DBF** is presented in Algorithm 1. Note that in this paper all the algorithms are written in PyTorch [48] style.

```

1  def forward(input):
2      out = model.backbone(input)
3      if freezing_scheduler(epoch): # proposed
4          out = out.detach()
5      if model.neck:
6          out = model.neck(out)
7      if model.roi_head:
8          out = model.roi_head(out)
9      out = model.bbox_head(out)
10     return out

```

ALGORITHM 1 Training with Dynamic Backbone Freezing.

A deep learning-based detector is typically composed of (a) a backbone network for feature extraction, (b) a neck for feature aggregation, and (c) a detection head for predicting bounding boxes and class scores. In Algorithm 1, `backbone` and `neck` correspond to (a) and (b), respectively. For (c), there are two types of heads: `roi_head` and `bbox_head`. In particular, `roi_head` is a specific type of (c) typically used in two-stage detectors like Faster R-CNN to refine the RoI (Region of Interest) proposals generated by the RPN (Region Proposal Network). Since some detectors may not have `neck` and `roi_head`, conditional statements are used to handle a runtime exception in lines 5 and 7 so that the proposed method is compatible with various architectures.

Table 1 Experimental configuration parameters in this work.

Dataset Backbone Scheduling policy	DOTA [13]				DIOR-R [14]			
	ResNet-50 [49] ~50 epochs	~400 epochs	Swin-S [50] ~400 epochs	~800 epochs	ResNet-50 [49] ~50 epochs	~200 epochs	Swin-S [50] ~400 epochs	~1600 epochs
(a) Full training	$\rho = 1$	$\rho = 1$	$\rho = 1$	$\rho = 1$	$\rho = 1$	$\rho = 1$	$\rho = 1$	$\rho = 1$
(b) Frozen Backbone [31]	$\rho = \infty$	$\rho = \infty$	$\rho = \infty$	$\rho = \infty$	$\rho = \infty$	$\rho = \infty$	$\rho = \infty$	$\rho = \infty$
(c) Ours (DBF)	$\rho = 1$	$\rho \in \{2, 5, 10, \infty\}$	$\rho = 1$	$\rho \in \{2, 5, 10, \infty\}$	$\rho = 1$	$\rho \in \{2, 5, 10, \infty\}$	$\rho = 1$	$\rho \in \{2, 5, 10, \infty\}$

Here, `forward()` defines the forward process of a detector model. It is the process of passing input data through the network to generate output. In this paper, we override this function for typical detector models with `freezing_scheduler` as shown in lines 3-4. If the condition of line 3 is true, `out` from `backbone` becomes detached in line 4, which means gradients for the backbone will not be computed, stopping the gradient flow to the backbone during back-propagation.

3.3 Design choice of Freezing Scheduler

The previous subsection centered on the basic pipeline of **DBF**. Nevertheless, we did not consider how to implement `freezing_scheduler` in code. This subsection aims to discuss the design principles of ‘Freezing Scheduler’.

This work assumes that the input to the Freezing Scheduler is the current epoch, and the output is a binary signal indicating whether the backbone should be frozen. Specifically, a signal of 0 allows backbone updates (i.e., unfreezes the backbone), while a signal of 1 freezes it. Using this scheduler, we can dynamically control the training process by alternating between freezing and unfreezing the backbone, as illustrated in Fig. 3. The flexibility of our framework enables researchers to design and implement various versions of the Freezing Scheduler according to their needs. Among these possible variants, we propose a simple yet effective approach called the “Step Freezing Scheduler,” which is described in Algorithm 2.

```

1 def freezing_scheduler(epoch):
2     # ρ: an integer greater than 1 and
3     # less than total epochs
4     if epoch % ρ == 0:
5         return 0          # unfreezing
6     return 1          # freezing

```

ALGORITHM 2 One of the simplest variants of Freezing Scheduler for **DBF** in this work: ‘Step Freezing Scheduler’.

Intuitively, our Step Freezing Scheduler is similar to a step learning rate scheduler [51] that decreases the learning rate at specific intervals based on the users’ demand during training. In Algorithm 2, ρ is the only hyper-parameter to be tuned by users. Our scheduler updates the feature backbone only every ρ epochs. In other words, a higher ρ value implies that the backbone remains frozen more frequently, leading to increased efficiency in GPU memory usage and faster training time. Moreover, it helps to preserve the pre-trained low-level generic knowledge in the backbone while simultaneously allowing the detection model to acquire domain-specific knowledge for more precise prediction.

4 Experiments

In this section, we show our novel feature backbone fine-tuning method, **DBF** enables more accurate model learning while significantly reducing computational costs under long-term training policies with CNN-based architectures for oriented object detection in remote sensing. Note that CNN-based detectors can embrace the transformer as a feature backbone.

4.1 Experimental setup

Baseline architectures. Deep learning models for object detection are conventionally split into one-stage and two-stage methods. Besides, anchor-based and anchor-free methods have been recently increasingly highlighted in the classification of detector models. In this study, we opted for Faster R-CNN [36], RetinaNet [52], and FCOS [33] as the representative models in anchor-based two-stage, anchor-based one-stage, and anchor-free one-stage object detection. For all benchmark models, we considered two exemplary neural networks as feature backbones: ResNet-50 [49] and Swin-S [50], one of the celebrated convolutional neural networks and transformer architectures, respectively. Moreover, FPN (Feature Pyramid Network)-1x [53] is used as a neck to enhance multi-scale invariance for our models. Here, we leverage ImageNet pre-trained weights for remote sensing object detection as they are still competitive baseline models to be readily online [21]. While alternative pre-trained models designed for remote sensing applications [19, 20] are available, they lack the ability to promptly adapt to novel network architectures. That is, for newly proposed neural networks, the weights trained on natural image datasets are more easily accessible. In contrast, those specialized in remote sensing imagery take considerable time to deploy. Thus, our experiments explore when the ImageNet pre-trained weights meet our method to boost remote sensing object detection.

Training details. We chose PyTorch and MMDetection [54] / MMrotate [55] for implementing our method and baseline architectures. For model optimization, SGD (Stochastic Gradient Descent) [56, 57] is used with momentum of weight 0.9, weight decay 0.0001, and batch size 8. The initial learning rate is set to 0.005 for all detectors. To enhance the stability and convergence of our training process, we utilize a linear learning rate warm-up strategy [58] over the initial 500 iterations, during which the learning rate increases linearly from zero to 33% of the maximum learning rate. The learning rate decayed by 1/4 after the 12th epoch. To prevent gradient explosion, L2 norm-based gradient clipping [59] is used with a maximum norm of 35. We apply the following data transformations for training: ‘¹RResize’, ‘²RRandomFlip’,

¹RResize is a rotation-aware resizing operation designed for resizing images and their associated oriented bounding boxes. For DOTA, it adapts the input to a predefined size, 1024x1024 while maintaining the aspect ratio. Similarly, for DIOR-R, it adjusts all inputs to a uniform target size, 800x800 while maintaining the aspect ratio. RResize is critical for efficient batching and optimized memory usage.

²RRandomFlip is a rotation-aware data augmentation technique that randomly flips images along specified axes (horizontal, vertical, or diagonal directions) while ensuring that the corresponding oriented bounding boxes are updated accordingly. For both DOTA and DIOR datasets, we consider all three directions with probability 0.25 in RRandomFlip.

Table 2 Experimental results on DOTA and DIOR-R with various convolutional object detection architectures (**Bold** text indicates the best while underlined text means the second-best in this paper). Notably, our method achieves higher validation mAP scores across nearly all cases for both datasets compared to approaches (a) and (b), underscoring its efficacy in long-term training scenarios for CNN-based object detection models in remote sensing.

Dataset	Detector	Backbone	(a) Full training (Baseline)		(b) Frozen Backbone [31]		(c) Ours (DBF)						
			mAP	Δ TFLOPs	mAP	Δ TFLOPs	($\rho = 1 \rightarrow$) $\rho = 2$	mAP	Δ TFLOPs	($\rho = 1 \rightarrow$) $\rho = 5$	mAP	Δ TFLOPs	($\rho = 1 \rightarrow$) $\rho = 10$
DOTA [13]	Faster R-CNN [36]	ResNet-50 [49]	69.00	61.31 (-7.69)	-3,077,501 (+0.03)	69.03 (+0.22)	-1,170,338	69.22 (+0.22)	-1,872,541	69.27 (+0.27)	-2,106,608	69.28 (+0.28)	-2,340,676
		Swin-S [50]	71.23	68.14 (-3.09)	-6,115,002 (+0.57)	71.80 (+0.50)	-1,538,750	71.73 (+0.50)	-2,462,001	71.74 (+0.51)	-2,769,751	71.73 (+0.50)	-3,077,501
	RetinaNet [52]	ResNet-50 [49]	64.19	57.29 (-6.90)	-3,077,501 (+0.29)	64.48 (+0.29)	-1,170,338	64.89 (+0.70)	-1,872,541	64.77 (+0.58)	-2,106,608	64.98 (+0.79)	-2,340,676
		Swin-S [50]	64.89	61.61 (-3.28)	-6,115,002 (+0.03)	64.92 (+0.13)	-1,538,750	65.02 (+0.13)	-2,462,001	65.01 (+0.12)	-2,769,751	64.97 (+0.08)	-3,077,501
DIOR-R [14]	FCOS [33]	ResNet-50 [49]	68.41	59.82 (-8.59)	-3,077,501 (+0.00)	68.41 (+0.39)	-1,170,338	68.80 (+0.39)	-1,872,541	68.98 (+0.57)	-2,106,608	69.18 (+0.77)	-2,340,676
		Swin-S [50]	71.47	67.45 (-4.02)	-6,115,002 (-0.01)	71.46 (-0.01)	-1,538,750	71.44 (-0.03)	-2,462,001	71.62 (+0.15)	-2,769,751	71.51 (+0.04)	-3,077,501
	Faster R-CNN [36]	ResNet-50 [49]	63.82	54.17 (-9.65)	-491,825 (+0.31)	64.13 (+0.03)	-184,434	63.85 (+0.03)	-295,095	63.86 (+0.04)	-331,982	63.96 (+0.14)	-368,869
		Swin-S [50]	67.68	62.64 (-5.04)	-4,588,368 (+0.29)	67.97 (+0.29)	-1,720,638	67.99 (+0.31)	-2,753,021	68.06 (+0.38)	-3,097,149	68.03 (+0.35)	-3,441,276
DIOR-R [14]	RetinaNet [52]	ResNet-50 [49]	59.09	53.88 (-5.21)	-491,825 (+0.17)	59.26 (+0.17)	-184,434	59.25 (+0.16)	-295,095	58.94 (-0.15)	-331,982	58.97 (-0.12)	-368,869
		Swin-S [50]	65.11	60.81 (-4.30)	-4,588,368 (+0.04)	65.15 (+0.03)	-1,720,638	65.14 (+0.03)	-2,753,021	64.86 (-0.25)	-3,097,149	64.75 (-0.36)	-3,441,276
	FCOS [33]	ResNet-50 [49]	61.23	55.84 (-5.39)	-491,825 (+0.16)	61.39 (+0.16)	-184,434	61.63 (+0.40)	-295,095	61.66 (+0.43)	-331,982	61.85 (+0.62)	-368,869
		Swin-S [50]	67.58	67.48 (-0.10)	-4,588,368 (+0.11)	67.69 (+0.11)	-1,720,638	68.08 (+0.50)	-2,753,021	68.05 (+0.47)	-3,097,149	68.05 (+0.47)	-3,441,276

and ‘³Normalize’ [55]. For a fair comparison, we set the value of the random seed to 0 during experiments.

To demonstrate the effectiveness of the proposed method, we compare it against (a) full training and (b) ‘Frozen Backbone’ [31]. In (a), the backbone is always fine-tuned every training epoch, which requires the highest computing resources. Meanwhile, in (b), the backbone is never fine-tuned (i.e. always frozen), leading to minimal resource usage. Our method balances the extremes of (a) and (b). Precisely, our approach can be seen as a generalized version of (a) and (b):

- If ρ equals 1, our method is equivalent to (a);
- If ρ equals ∞ , our method is equivalent to (b).

Table 1 indicates the experimental configuration parameters in this work. As mentioned in Sec. 3.3, we use Step Freezing Scheduler for **DBF**. Besides, we consider four ρ values, $\{2, 5, 10, \infty\}$ in our method: the models fully fine-tuned (i.e. $\rho = 1$) for the first 50 or 400 epochs are fine-tuned again with **DBF** under the four ρ values.

4.2 Evaluation metrics

mAP (mean Average Precision) is a key metric used to evaluate the accuracy of object localization and classification. We adopt mAP to provide a balanced assessment of models with both precision and recall across different categories in multiple object detection. Assume that TP means true positives, FP means false positives, and

³All images are normalized per each color channel (R/G/B) with means [123.68, 116.28, 103.53] and standard deviations [58.40, 57.12, 57.38].

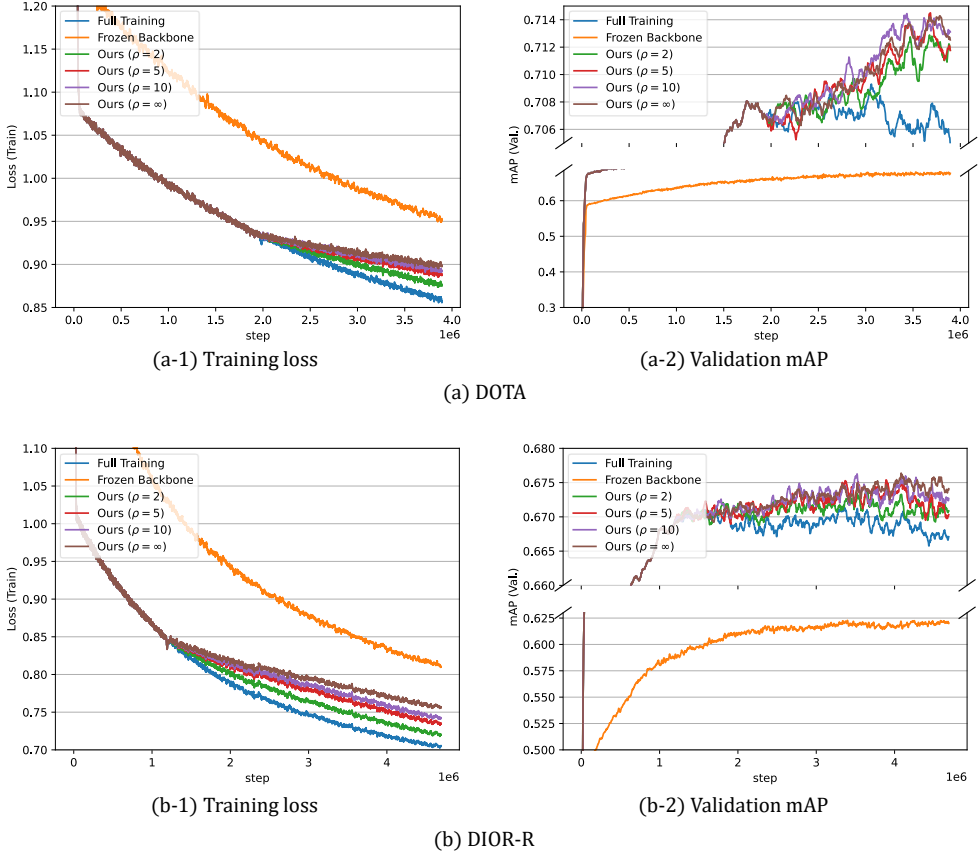


Fig. 4 Learning curves on DOTA and DIOR-R with Faster R-CNN and Swin-S: It can be seen that while our **DBF** shows slower training loss reduction than ‘Full training’, it shows stable and highest validation mAP values. Particularly, the validation mAP consistently shows an upward trend when using our method under long-term training scenarios. In the case of ‘Frozen Backbone’, while it incurs the lowest training cost, there is a considerable degradation in model performance compared to other approaches.

FN means false negatives. Precision is the proportion of predicted objects that are correctly identified as follows:

$$\text{Precision} = \frac{\text{TP}}{\text{TP} + \text{FP}}. \quad (1)$$

Recall is the proportion of actual objects correctly detected by the model as:

$$\text{Recall} = \frac{\text{TP}}{\text{TP} + \text{FN}}. \quad (2)$$

We recommend to see [60] for detailed calculation of mAP.

Precisely, ‘mAP@50’ [61] is used for model evaluation following [47]. In mAP@50, predictions with $\text{IoU} \geq 0.5$ are considered correct, where IoU (Intersection over Union) per each prediction is calculated as follows:

$$\text{IoU} = \frac{\text{Area of overlap between } \hat{y} \text{ and } y}{\text{Area of union}}, \quad (3)$$

where \hat{y} is the predicted bounding box and y is the ground truth bounding box.

FLOPs (FLoating point OPerations) refers to the total number of floating-point operations performed by a model during training or inference. It represents the computational cost of a model. Matrix multiplications and additions contribute to the FLOPs count during input propagation through the model. Typically, FLOPs are calculated based solely on the one forward pass with a batch size of 1 [62].

On the other side, we use F_{total} instead as follows:

$$F_{\text{total}} = \sum_{e=1}^E \sum_{i=1}^N \sum_{l=1}^L (F_{\text{forward}}(e, l) + F_{\text{backward}}(e, l)), \quad (4)$$

where E is total training epochs, N is the number of training samples, and L is the number of network layers. $F_{\text{forward}}(e, l)$ and $F_{\text{backward}}(e, l)$ correspond to FLOPs for forward and backward operations at the e -th epoch in the l -th layer, respectively. During computation, F_{forward} only focuses on the input, whereas F_{backward} takes into account the weights and inputs for gradient flow. Hence, this work assumes that F_{backward} is twice that of F_{forward} . Intuitively, ΔF_{total} effectively shows how much computation reduces during all training epochs.

4.3 Datasets

We perform experiments on the following datasets for generic multiple object detection in remote sensing: DOTA-v1.0 [13] and DIOR-R [14]. For our experiments, we only consider labels for oriented object detection, as detecting rotated objects is more practical in remote sensing. DOTA consists of 15 object categories including ‘car’, ‘ship’, and ‘harbor’, with 2,806 aerial images and 188,282 bounding box labels. DIOR-R surpasses DOTA with its 20 object categories and 192,512 instances captured in 23,463 images. Note that we adopt standard training and test protocols for both datasets following prior researches like [47].

4.4 Experimental results

As seen in Table 2, our method performs better in most cases for all datasets. Here, ΔTFLOPs denotes the difference in Tera FLOPs relative to the baseline (a). In other words, the lower ΔTFLOPs , the better. As mentioned before, the FLOPs should be calculated as F_{total} in Eq. 4. Besides, ‘ $(\rho = 1 \rightarrow) \rho = \alpha$ ’ in (c) means that the backbone is fine-tuned with $\rho = 1$ for the first 50 or 400 epochs and then fine-tuned again with $\rho = \alpha$ according to Table 1. Although (a) permits adjusting the backbone for every epoch, it mostly results in slightly lower mAP than ours. Besides, (b) decreases ΔTFLOPs the most, but it undergoes a significant drop in mAP (about 3 to 10%).

Table 3 Examples of training time savings on Nvidia RTX A5000. Although long-term training usually entails significant computational time and memory usage, the proposed approach enables a more efficient process with reduced resource requirements. Remarkably, it achieves this while delivering superior inference accuracy.

FCOS + ResNet-50 on DOTA	Training policy		mAP	Δ TFLOPs	Training Time (T)	ΔT
	~50 epochs	~400 epochs				
(a) Full training	$\rho = 1$	$\rho = 1$	68.41	-	9,200m	-
(b) Frozen Backbone	$\rho = \infty$	$\rho = \infty$	59.82	-3,077,501	6,400m	-2,800m
(c) Ours	$\rho = 1$	$\rho = 2$	68.41	-1,170,338	7,975m	-1,225m
	$\rho = 1$	$\rho = 5$	68.80	-1,872,541	7,240m	-1,960m
	$\rho = 1$	$\rho = 10$	68.98	-2,106,608	6,995m	-2,205m
	$\rho = 1$	$\rho = \infty$	69.18	-2,340,676	<u>6,750m</u>	<u>-2,450m</u>

Compared to (a) and (b), the proposed approach balances low time complexity and precise inference ability: our method achieves the highest mAP for almost all cases, while effectively reducing computational costs during training.

To discuss the practical effectiveness of the proposed technique, we present how much training time can be saved when adopting our approach. Let the detector be FCOS with ResNet-50 as a backbone. For the training split of DOTA, using the Nvidia RTX A5000, it takes an average of 23 minutes to fully fine-tune the model, including the backbone, in one epoch. Freezing the backbone takes 16 minutes on average. Based on these, we can approximately calculate the training time for each training policy as shown in Table 3.

Here, ΔT means the difference in training time compared to (a). Interestingly, ours with $\rho = \infty$ achieves a 0.77 higher mAP while reducing the training time by 2,450 minutes (1.7 days) compared to the baseline. Reducing model learning time by several days or months holds significant benefits as:

- *Cost reduction*: Cutting down on training time can significantly lower cloud usage costs and power bills;
- *Productivity improvement*: Shorter training times enable more experiments (e.g. hyper-parameter tuning or ablation study) to be conducted quickly;
- *Sustainable AI*: Lower power consumption for model training translates to reduced carbon emissions, leading to environmental conservation and eco-friendly AI.

Fig. 4 further demonstrates the effectiveness of the proposed method. In all sub-figures, a downward trend is visible in the validation mAP curves for (a) full training, while the training loss also decreases the fastest, indicating over-fitting. On the other hand, the proposed method gradually reduces the training loss while improving the validation mAP, or at least preventing it from decreasing, especially for higher ρ . These observations show that the proposed method helps in stable model convergence while reducing memory usage.

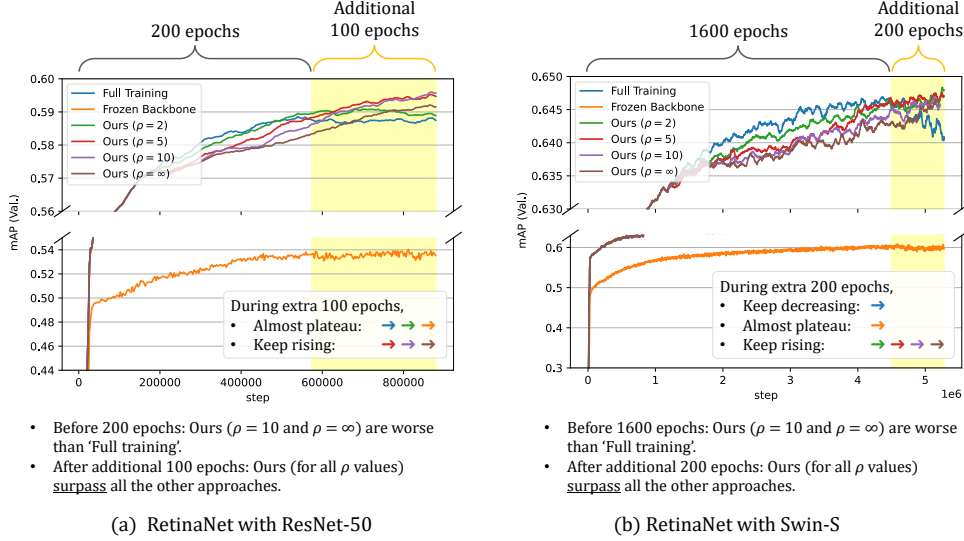


Fig. 5 Effects of further training of the proposed method for RetinaNet on DIOR-R: It can be confirmed that though our **DBF** achieves worse mAP than the baseline when $\rho \in \{10, \infty\}$ during the initial training following the policies in Table 1, the prediction accuracy of ours are eventually improved with longer additional training. Besides, it brings steady performance improvement even in long-term training, compared to other methods.

4.5 Parameter study of ρ

This subsection examines how users can effectively select ρ value. In the experiments, we consider four ρ values, $\{2, 5, 10, \infty\}$ for our method. One certain thing is that as the ρ value increases, more time and memory are saved in training. However, larger ρ deprives the learning opportunity of the feature backbone, which might hurt the model generalization. To find the best ρ , we compute the average of ΔmAP over all the experiments for each ρ . Table 4 indicates that $\rho = \infty$ is the optimal choice and the correlation between ρ and the improvement in model performance is evident.

Table 4 Average of ΔmAP for each ρ in **DBF**.

ΔmAP	$\rho = 2$	$\rho = 5$	$\rho = 10$	$\rho = \infty$
mean \pm standard deviation	0.17 ± 0.2	0.28 ± 0.2	0.27 ± 0.3	0.30 ± 0.3

4.6 Weakness analysis

Although our approach usually achieves competitive performance on several benchmarks and detectors, a relatively larger performance drop (-0.12 to -0.36) can be

observed on the DIOR-R dataset when ρ is greater than 10 for the RetinaNet architecture as shown in Table 1. Fortunately, this is not a limitation of the proposed method but because we terminate training early following the pre-fixed policy in Table 1, even though the model has not converged sufficiently. As shown in Fig 5, our method surpasses the other approaches for all ρ values when we additionally train the models with ResNet-50 and Swin-S for 100 and 200 epochs more, respectively. Remark that we attempted to train more than 100 or 200 epochs for each case; but, we observed that the performance of all methods either deteriorated or showed no improvement, so we ceased further training.

Despite the success of our method, current work has notable weaknesses. First, the optimal ρ value is not always fixed. As indicated in Table 2, $\rho = \infty$ is not the optimal for some cases. For instance, in Faster R-CNN with ResNet-50, the mean Average Precision gradually increases as ρ goes to ∞ for DOTA ($+0.03 \rightarrow +0.22 \rightarrow +0.27 \rightarrow 0.28$), whereas for DIOR-R, a U-shaped mAP trend is observed ($+0.31 \rightarrow +0.03 \rightarrow +0.04 \rightarrow +0.14$). To address this, future work would include exploring more diverse freezing schedulers that automatically decide whether to update the backbone based on input samples or learning curves online.

Besides, there is still room for further improvement in our method, in terms of training cost. For example, Adapters [9] for NLP can be leveraged in our method to boost more efficient fine-tuning without updating the entire backbone.

5 Comparison with state-of-the-art methods

In Section 4, DBF has proven to be an efficient fine-tuning strategy for long-term training in CNN-based remote sensing object detection models. To further validate its effectiveness, we extend our experiments by incorporating DBF into a state-of-the-art end-to-end transformer-based object detection model, OrientedFormer [3]. In this section, we also include a comparison with state-of-the-art methods, for comparative evaluation.

5.1 Experimental setup

In this section, we choose OrientedFormer [3] as the representative end-to-end transformer-based object detection models in remote sensing. In addition, we opt for a DIOR-R dataset, one of the well-known large-scale datasets for oriented object detection in remote sensing. Following [3], we use the same data augmentation strategies for DIOR-R, as mentioned in Section 4. To show the accuracy of our method, we use ‘mAP@50’ as an evaluation metric, as in Section 4.2. In the original paper [3], the model is trained for 12 epochs with the image size 800x800 with DIOR-R. However, we train the model for 250 epochs with the proposed fine-tuning approach. In the previous section, we observed ‘ $(\rho = 1 \rightarrow) \rho = \infty$ ’ in DBF is the optimal choice under long-term training. Hence, we set ρ as 1 for first 50 epochs, and then ∞ for the remaining 200 epochs.

Table 5 Comparison with state-of-the-art oriented object detection models on DIOR-R. Here, OrientedFormer, combined with our training scheme, achieves the best mAP, demonstrating the effectiveness of the proposed method.

Detector	Backbone	mAP
One-stage:		
RetinaNet (ICCV 2017) [52]	ResNet-50 [49]	57.55
DFNet (IEEE TGRS 2024) [63]	ResNet-50 [49]	62.11
Oriented Rep (CVPR 2022) [34]	ResNet-50 [49]	66.71
DCFL (CVPR 2023) [64]	ResNet-50 [49]	66.80
Two-stage:		
Gliding Vertex (IEEE TPAMI 2020) [65]	ResNet-50 [49]	60.06
RoI Transformer (CVPR 2019) [66]	ResNet-50 [49]	63.87
QPDet (IEEE TGRS 2023) [67]	ResNet-50 [49]	64.20
AOPG (IEEE TGRS 2022) [14]	ResNet-50 [49]	64.41
DODet (IEEE TGRS 2022) [68]	ResNet-50 [49]	65.10
End-to-end:		
ARS-DETR (IEEE TGRS 2024) [69]	ResNet-50 [49]	66.12
OrientedFormer (IEEE TGRS 2024) [3]	Swin-S [50]	68.84
OrientedFormer [3] + DBF (Ours)	Swin-S [50]	69.38 (+0.54)

5.2 Experimental results

We compare our approach against both recent CNN-based and transformer-based detectors on DIOR-R. As indicated in Table 5, our approach achieves 69.38%, surpassing all compared CNN-based one-stage and two-stage detectors as well as end-to-end transformer-based detectors. Specifically, our method improves upon the baseline OrientedFormer model by +0.54 mAP, demonstrating the effectiveness of integrating Dynamic Backbone Freezing (DBF) for enhanced performance in remote sensing object detection tasks.

6 Conclusions and future work

In this paper, we have proposed a simple but efficient backbone fine-tuning strategy named DBF for the remote sensing object detection. This work demonstrated that alternating between freezing and unfreezing the backbone aids remote sensing object detection models in learning both general and domain-specific knowledge under long-term training. Particularly with the proposed method, a significant decrease in memory usage and training time can be achieved under very long training schedules. Our approach has shown powerful results on DOTA and DIOR-R datasets with various detection architectures. Additionally, the intuitive design of DBF guarantees high compatibility with current deep learning frameworks, facilitating easy comprehension and seamless integration.

In the future, more sophisticated studies will be conducted as follows: (i) connecting the current method with the backbone initialized with other remote sensing

pre-training methodologies like [19, 20] rather than ImageNet-based one; (ii) extending this work to other remote sensing understanding tasks such as segmentation and change detection; (iii) designing novel freezing schedulers to mitigate class imbalance issues [70] under long-term training. We believe these research directions are crucial for future work.

Author contributions. JP and YK: Data curation, conceptualization, methodology and experimenting. MJ: Methodology and supervision.

Funding. This work was supported by the Agency For Defense Development Grant funded by the Korean Government (UI220066WD).

Availability of data and materials. Not applicable.

Code availability. Our code will be released on GitHub after our paper is accepted.

Declarations

Ethics approval and consent to participate. Not applicable.

Consent for publication. Not applicable.

Competing interests. The authors declare that they have no known competing financial interests or personal relationships that could have appeared to influence the work reported in this paper.

References

- [1] Lee, Y., Kim, Y., Yu, J., Jeon, M.: Learning to remove bad weather: towards robust visual perception for self-driving. *IEEE Robotics and Automation Letters* (2022)
- [2] Lee, Y., Ko, Y., Kim, Y., Jeon, M.: Perception-friendly video enhancement for autonomous driving under adverse weather conditions. In: 2022 International Conference on Robotics and Automation (ICRA), pp. 7760–7767 (2022). IEEE
- [3] Zhao, J., Ding, Z., Zhou, Y., Zhu, H., Du, W.-L., Yao, R., El Saddik, A.: Orientedformer: An end-to-end transformer-based oriented object detector in remote sensing images. *IEEE Transactions on Geoscience and Remote Sensing* (2024)
- [4] Deng, J., Dong, W., Socher, R., Li, L.-J., Li, K., Fei-Fei, L.: Imagenet: A large-scale hierarchical image database. In: 2009 IEEE Conference on Computer Vision and Pattern Recognition, pp. 248–255 (2009). Ieee
- [5] Beyer, L., Zhai, X., Royer, A., Markeeva, L., Anil, R., Kolesnikov, A.: Knowledge distillation: A good teacher is patient and consistent. In: Proceedings of the IEEE/CVF Conference on Computer Vision and Pattern Recognition, pp. 10925–10934 (2022)

- [6] Kim, Y., Kim, S., Jeon, M.: Nbbox: Noisy bounding box improves remote sensing object detection. *IEEE Geoscience and Remote Sensing Letters* (2025)
- [7] Kim, Y., Yoon, D., Kim, S., Jeon, M.: Nsegment: Label-specific deformations for remote sensing image segmentation. *IEEE Geoscience and Remote Sensing Letters* (2025)
- [8] Kim, Y., Yoon, D., Lee, Y., Fatima, U., Kim, H.K., Lee, S., Park, S., Park, J.H., Kang, S., Jeon, M.: Unlocking robust semantic segmentation performance via label-only elastic deformations against implicit label noise. *arXiv preprint arXiv:2508.10383* (2025)
- [9] Houlsby, N., Giurgiu, A., Jastrzebski, S., Morrone, B., De Laroussilhe, Q., Gesmundo, A., Attariyan, M., Gelly, S.: Parameter-efficient transfer learning for nlp. In: *International Conference on Machine Learning*, pp. 2790–2799 (2019). PMLR
- [10] Li, X.L., Liang, P.: Prefix-tuning: Optimizing continuous prompts for generation. *arXiv preprint arXiv:2101.00190* (2021)
- [11] Hu, E.J., Shen, Y., Wallis, P., Allen-Zhu, Z., Li, Y., Wang, S., Wang, L., Chen, W.: Lora: Low-rank adaptation of large language models. *arXiv preprint arXiv:2106.09685* (2021)
- [12] Lester, B., Al-Rfou, R., Constant, N.: The power of scale for parameter-efficient prompt tuning. *arXiv preprint arXiv:2104.08691* (2021)
- [13] Xia, G.-S., Bai, X., Ding, J., Zhu, Z., Belongie, S., Luo, J., Datcu, M., Pelillo, M., Zhang, L.: Dota: A large-scale dataset for object detection in aerial images. In: *Proceedings of the IEEE Conference on Computer Vision and Pattern Recognition*, pp. 3974–3983 (2018)
- [14] Cheng, G., Wang, J., Li, K., Xie, X., Lang, C., Yao, Y., Han, J.: Anchor-free oriented proposal generator for object detection. *IEEE Transactions on Geoscience and Remote Sensing* **60**, 1–11 (2022)
- [15] Wang, D., Zhang, J., Du, B., Xia, G.-S., Tao, D.: An empirical study of remote sensing pretraining. *IEEE Transactions on Geoscience and Remote Sensing* **61**, 1–20 (2022)
- [16] Fuller, A., Millard, K., Green, J.R.: Satvit: Pretraining transformers for earth observation. *IEEE Geoscience and Remote Sensing Letters* **19**, 1–5 (2022)
- [17] Reed, C.J., Gupta, R., Li, S., Brockman, S., Funk, C., Clipp, B., Keutzer, K., Candido, S., Uyttendaele, M., Darrell, T.: Scale-mae: A scale-aware masked autoencoder for multiscale geospatial representation learning. In: *Proceedings of the IEEE/CVF International Conference on Computer Vision*, pp. 4088–4099 (2023)

- [18] Zhang, T., Zhuang, Y., Chen, H., Chen, L., Wang, G., Gao, P., Dong, H.: Object-centric masked image modeling-based self-supervised pretraining for remote sensing object detection. *IEEE Journal of Selected Topics in Applied Earth Observations and Remote Sensing* **16**, 5013–5025 (2023)
- [19] Huang, Z., Zhang, M., Gong, Y., Liu, Q., Wang, Y.: Generic knowledge boosted pre-training for remote sensing images. *IEEE Transactions on Geoscience and Remote Sensing* (2024)
- [20] Wang, D., Zhang, J., Xu, M., Liu, L., Wang, D., Gao, E., Han, C., Guo, H., Du, B., Tao, D., et al.: Mtp: Advancing remote sensing foundation model via multi-task pretraining. *IEEE Journal of Selected Topics in Applied Earth Observations and Remote Sensing* (2024)
- [21] Corley, I., Robinson, C., Dodhia, R., Ferres, J.M.L., Najafirad, P.: Revisiting pre-trained remote sensing model benchmarks: resizing and normalization matters. In: *Proceedings of the IEEE/CVF Conference on Computer Vision and Pattern Recognition*, pp. 3162–3172 (2024)
- [22] Fuller, A., Millard, K., Green, J.: Croma: Remote sensing representations with contrastive radar-optical masked autoencoders. *Advances in Neural Information Processing Systems* **36** (2024)
- [23] Liu, N., Xu, X., Gao, Y., Zhao, Y., Li, H.-C.: Semi-supervised object detection with uncurated unlabeled data for remote sensing images. *International Journal of Applied Earth Observation and Geoinformation* **129**, 103814 (2024)
- [24] Liu, N., Xu, X., Celik, T., Gan, Z., Li, H.-C.: Transformation-invariant network for few-shot object detection in remote-sensing images. *IEEE Transactions on Geoscience and Remote Sensing* **61**, 1–14 (2023)
- [25] Liu, N., Xu, X., Su, Y., Zhang, H., Li, H.-C.: Pointsam: Pointly-supervised segment anything model for remote sensing images. *IEEE Transactions on Geoscience and Remote Sensing* (2025)
- [26] Gao, T., Li, Z., Wen, Y., Chen, T., Niu, Q., Liu, Z.: Attention-free global multiscale fusion network for remote sensing object detection. *IEEE transactions on geoscience and remote sensing* **62**, 1–14 (2023)
- [27] Li, Z., Gao, T., An, Y., Chen, T., Zhang, J., Wen, Y., Liu, M., Zhang, Q.: Brain-inspired spiking neural networks for energy-efficient object detection. In: *Proceedings of the Computer Vision and Pattern Recognition Conference*, pp. 3552–3562 (2025)
- [28] Rebuffi, S.-A., Bilen, H., Vedaldi, A.: Learning multiple visual domains with residual adapters. *Advances in neural information processing systems* **30** (2017)

- [29] Rebuffi, S.-A., Bilen, H., Vedaldi, A.: Efficient parametrization of multi-domain deep neural networks. In: Proceedings of the IEEE Conference on Computer Vision and Pattern Recognition, pp. 8119–8127 (2018)
- [30] Lin, Y., Liu, Z., Zhang, Z., Hu, H., Zheng, N., Lin, S., Cao, Y.: Could giant pre-trained image models extract universal representations? Advances in Neural Information Processing Systems **35**, 8332–8346 (2022)
- [31] Vasconcelos, C., Birodkar, V., Dumoulin, V.: Proper reuse of image classification features improves object detection. In: Proceedings of the IEEE/CVF Conference on Computer Vision and Pattern Recognition, pp. 13628–13637 (2022)
- [32] Wen, L., Cheng, Y., Fang, Y., Li, X.: A comprehensive survey of oriented object detection in remote sensing images. Expert Systems with Applications **224**, 119960 (2023)
- [33] Detector, A.-F.O.: Fcos: a simple and strong anchor-free object detector. IEEE Transactions on Pattern Analysis and Machine Intelligence **44**(4) (2022)
- [34] Li, W., Chen, Y., Hu, K., Zhu, J.: Oriented repoints for aerial object detection. In: Proceedings of the IEEE/CVF Conference on Computer Vision and Pattern Recognition, pp. 1829–1838 (2022)
- [35] Guo, Z., Liu, C., Zhang, X., Jiao, J., Ji, X., Ye, Q.: Beyond bounding-box: Convex-hull feature adaptation for oriented and densely packed object detection. In: Proceedings of the IEEE/CVF Conference on Computer Vision and Pattern Recognition, pp. 8792–8801 (2021)
- [36] Ren, S., He, K., Girshick, R., Sun, J.: Faster r-cnn: Towards real-time object detection with region proposal networks. IEEE transactions on pattern analysis and machine intelligence **39**(6), 1137–1149 (2016)
- [37] Xie, X., Cheng, G., Wang, J., Yao, X., Han, J.: Oriented r-cnn for object detection. In: Proceedings of the IEEE/CVF International Conference on Computer Vision, pp. 3520–3529 (2021)
- [38] Han, J., Ding, J., Xue, N., Xia, G.-S.: Redet: A rotation-equivariant detector for aerial object detection. In: Proceedings of the IEEE/CVF Conference on Computer Vision and Pattern Recognition, pp. 2786–2795 (2021)
- [39] Carion, N., Massa, F., Synnaeve, G., Usunier, N., Kirillov, A., Zagoruyko, S.: End-to-end object detection with transformers. In: European Conference on Computer Vision, pp. 213–229 (2020). Springer
- [40] Zhu, X., Su, W., Lu, L., Li, B., Wang, X., Dai, J.: Deformable detr: Deformable transformers for end-to-end object detection. arXiv preprint arXiv:2010.04159 (2020)

- [41] Zhou, Y., Chen, S., Zhao, J., Yao, R., Xue, Y., El Saddik, A.: Clt-det: Correlation learning based on transformer for detecting dense objects in remote sensing images. *IEEE Transactions on Geoscience and Remote Sensing* **60**, 1–15 (2022)
- [42] Dai, L., Liu, H., Tang, H., Wu, Z., Song, P.: Ao2-detr: Arbitrary-oriented object detection transformer. *IEEE Transactions on Circuits and Systems for Video Technology* **33**(5), 2342–2356 (2022)
- [43] Zhou, Q., Yu, C., Wang, Z., Wang, F.: D 2 q-detr: Decoupling and dynamic queries for oriented object detection with transformers. In: ICASSP 2023-2023 IEEE International Conference on Acoustics, Speech and Signal Processing (ICASSP), pp. 1–5 (2023). IEEE
- [44] Chen, K., Liu, C., Chen, B., Li, W., Zou, Z., Shi, Z.: Dynamicvis: An efficient and general visual foundation model for remote sensing image understanding. arXiv preprint arXiv:2503.16426 (2025)
- [45] Chen, K., Liu, C., Chen, H., Zhang, H., Li, W., Zou, Z., Shi, Z.: Rsprompter: Learning to prompt for remote sensing instance segmentation based on visual foundation model. *IEEE Transactions on Geoscience and Remote Sensing* **62**, 1–17 (2024)
- [46] Chen, K., Liu, C., Chen, B., Zhang, J., Zou, Z., Shi, Z.: Rsrefseg 2: Decoupling referring remote sensing image segmentation with foundation models. arXiv preprint arXiv:2507.06231 (2025)
- [47] Li, C., Cheng, G., Wang, G., Zhou, P., Han, J.: Instance-aware distillation for efficient object detection in remote sensing images. *IEEE Transactions on Geoscience and Remote Sensing* **61**, 1–11 (2023)
- [48] Paszke, A., Gross, S., Massa, F., Lerer, A., Bradbury, J., Chanan, G., Killeen, T., Lin, Z., Gimelshein, N., Antiga, L., et al.: Pytorch: An imperative style, high-performance deep learning library. *Advances in neural information processing systems* **32** (2019)
- [49] He, K., Zhang, X., Ren, S., Sun, J.: Deep residual learning for image recognition. In: Proceedings of the IEEE Conference on Computer Vision and Pattern Recognition, pp. 770–778 (2016)
- [50] Liu, Z., Lin, Y., Cao, Y., Hu, H., Wei, Y., Zhang, Z., Lin, S., Guo, B.: Swin transformer: Hierarchical vision transformer using shifted windows. In: Proceedings of the IEEE/CVF International Conference on Computer Vision, pp. 10012–10022 (2021)
- [51] Ge, R., Kakade, S.M., Kidambi, R., Netrapalli, P.: The step decay schedule: A near optimal, geometrically decaying learning rate procedure for least squares. *Advances in neural information processing systems* **32** (2019)

- [52] Ross, T.-Y., Dollár, G.: Focal loss for dense object detection. In: Proceedings of the IEEE Conference on Computer Vision and Pattern Recognition, pp. 2980–2988 (2017)
- [53] Lin, T.-Y., Dollár, P., Girshick, R., He, K., Hariharan, B., Belongie, S.: Feature pyramid networks for object detection. In: Proceedings of the IEEE Conference on Computer Vision and Pattern Recognition, pp. 2117–2125 (2017)
- [54] Chen, K., Wang, J., Pang, J., Cao, Y., Xiong, Y., Li, X., Sun, S., Feng, W., Liu, Z., Xu, J., et al.: Mmdetection: Open mmlab detection toolbox and benchmark. arXiv preprint arXiv:1906.07155 (2019)
- [55] Zhou, Y., Yang, X., Zhang, G., Wang, J., Liu, Y., Hou, L., Jiang, X., Liu, X., Yan, J., Lyu, C., et al.: Mmrotate: A rotated object detection benchmark using pytorch. In: Proceedings of the 30th ACM International Conference on Multimedia, pp. 7331–7334 (2022)
- [56] Amari, S.-i.: Backpropagation and stochastic gradient descent method. *Neurocomputing* **5**(4-5), 185–196 (1993)
- [57] Zinkevich, M., Weimer, M., Li, L., Smola, A.: Parallelized stochastic gradient descent. *Advances in neural information processing systems* **23** (2010)
- [58] Kalra, D.S., Barkeshli, M.: Why warmup the learning rate? underlying mechanisms and improvements. arXiv preprint arXiv:2406.09405 (2024)
- [59] Zhang, J., He, T., Sra, S., Jadbabaie, A.: Why gradient clipping accelerates training: A theoretical justification for adaptivity. arXiv preprint arXiv:1905.11881 (2019)
- [60] Wang, B.: A parallel implementation of computing mean average precision. arXiv preprint arXiv:2206.09504 (2022)
- [61] Everingham, M., Eslami, S.A., Van Gool, L., Williams, C.K., Winn, J., Zisserman, A.: The pascal visual object classes challenge: A retrospective. *International journal of computer vision* **111**, 98–136 (2015)
- [62] Johnson, J.: Rethinking floating point for deep learning. arxiv preprint arXiv:1811.01721 (2018)
- [63] Xie, X., Cheng, G., Rao, C., Lang, C., Han, J.: Oriented object detection via contextual dependence mining and penalty-incentive allocation. *IEEE Transactions on Geoscience and Remote Sensing* (2024)
- [64] Xu, C., Ding, J., Wang, J., Yang, W., Yu, H., Yu, L., Xia, G.-S.: Dynamic coarse-to-fine learning for oriented tiny object detection. In: Proceedings of the IEEE/CVF Conference on Computer Vision and Pattern Recognition, pp.

- [65] Xu, Y., Fu, M., Wang, Q., Wang, Y., Chen, K., Xia, G.-S., Bai, X.: Gliding vertex on the horizontal bounding box for multi-oriented object detection. *IEEE transactions on pattern analysis and machine intelligence* **43**(4), 1452–1459 (2020)
- [66] Ding, J., Xue, N., Long, Y., Xia, G.-S., Lu, Q.: Learning roi transformer for oriented object detection in aerial images. In: *Proceedings of the IEEE/CVF Conference on Computer Vision and Pattern Recognition*, pp. 2849–2858 (2019)
- [67] Yao, Y., Cheng, G., Wang, G., Li, S., Zhou, P., Xie, X., Han, J.: On improving bounding box representations for oriented object detection. *IEEE Transactions on Geoscience and Remote Sensing* **61**, 1–11 (2022)
- [68] Cheng, G., Yao, Y., Li, S., Li, K., Xie, X., Wang, J., Yao, X., Han, J.: Dual-aligned oriented detector. *IEEE Transactions on Geoscience and Remote Sensing* **60** (2022)
- [69] Zeng, Y., Chen, Y., Yang, X., Li, Q., Yan, J.: Ars-detr: Aspect ratio-sensitive detection transformer for aerial oriented object detection. *IEEE Transactions on Geoscience and Remote Sensing* **62**, 1–15 (2024)
- [70] Kim, Y., Lee, Y., Jeon, M.: Imbalanced image classification with complement cross entropy. *Pattern Recognition Letters* **151**, 33–40 (2021)